Chapter

Adsorption of Heavy Metals on Layered Double Hydroxides (LDHs) Intercalated with Chelating Agents

Naoki Kano and Shuang Zhang

Abstract

Layered double hydroxides (LDHs) are lamellar ionic compounds containing a positively charged layer and exchangeable anions in the interlayer. In this study, LDHs intercalated with chelating agents were synthesized by anion exchange reaction. The materials synthesized in this work were characterized by chemical analysis, Fourier transform infrared spectroscopy (FT-IR), scanning electron microscopy (SEM), and powder X-ray diffraction (XRD) to confirm their properties. Adsorption experiments from aqueous solutions containing known amounts of some heavy metallic ions onto the adsorbent were explored in a batch system. The amount of metallic ions adsorbed by LDHs intercalated with EDTA and precursor LDHs were determined by inductively coupled plasma-atomic emission spectrometry (ICP-AES) and atomic absorption spectrometry (AAS). In order to examine the adsorption capacity of LDHs intercalated with chelating agents, the adsorption experiment was investigated under the optimum condition. The data were applied to Langmuir and Freundlich isotherm models. The pseudo-second-order kinetic model was more adequate to describe the kinetic in this case. LDHs intercalated with chelating agents synthesized in this work can be promising adsorbents for heavy metals. It is very significant information from the viewpoint of environmental protection.

Keywords: adsorption, layered double hydroxides (LDHs), chelating agent, heavy metals, adsorption isotherms, kinetics

1. Introduction

Recently, environmental pollution is one of the most serious problems in the world due to its deep effect on the future of human beings. Then the investigation for resolving the problem of the environmental pollution in the world began to draw major public attention [1, 2]. It is well known that the major forms of environmental pollution include air pollution, water pollution, soil pollution, and so on. Among them, water pollution is the most serious due to its liquidity which may bring other pollutions. Surface water pollution and groundwater contamination are some of the environmental problems today. One of the cases of environmental pollution is due to heavy metal contaminants such as copper, lead, cadmium, chromium, arsenic, zinc, etc. Also, heavy metals are concerned because of their strong toxicity even at

low concentrations. Based on the type of mining, the kinds and the concentrations of metal ions are many and varied. Heavy metal ions have high toxicity and poor biodegradability for plants and animals at higher concentrations [3, 4].

In recent years, clay minerals have been aroused increasing interest as adsorbents by virtue of their properties, which make them attractive materials for adsorbing heavy metal ions. Their abundance in nature, low cost, and good cation adsorptive properties, a result of their negatively charged layers and high specific surface areas, make them suitable for adsorption of metal ions [5, 6]. LDH used in this paper are the antitypes of clay minerals. Layered double hydroxides (LDHs) are lamellar ionic compounds containing a positively charged layer and exchangeable anions in the interlayer. They consist of brucite-like layers and are represented by the general formula $[M^{II}_{1-x}M^{III}_{x}(OH)_2](A^{n-})_{x/n}\cdot mH_2O$, where cationic M^{II} and M^{III} are divalent and trivalent metals and occupy the octahedral holes in the brucite-like layer. An^- is the interlayer exchangeable anions, which is located in the hydrate layered galleries, and x is the layer charge density $x = [M^{II}]/([M^{III}] + [M^{III}])$ [7–9]. The layered structure of LDHs is shown in **Figure 1**.

The ethylenediaminetetraacetic acid (EDTA) is a chelating agent widely used in industry and agriculture. It forms strong complexes with the ratio 1:1 between heavy metal ions and ligand. The EDDS (N, N′-1, 2-Ethanediylbis-1-Aspartic Acid) is also a chelating agent, which may offer a biodegradable alternative to EDTA and is currently used on a large scale in numerous applications [10, 11]. The structure of this two chelating agents were shown in **Figure 2**.

Considering the structure of LDHs, it is suggested that these compounds can be intercalated with different polydentate ligands. Recently, the study using LDHs modified with chelating agents as the potential adsorbents of heavy metals from aqueous solution has been reported [12, 13]. The aim of this work is at first to synthesize and to characterize LDHs intercalated with EDTA or EDDS and to study the uptake of heavy metals (Cu^{2+}, Pb^{2+}, Cd^{2+}) by these hybrid compounds. The following five kinds of compounds synthesized in this work are ZnAl-NO_3 (L1), ZnAl-EDTA (L2), MgAl-NO_3 (L3), MgAl-EDTA (L4), and MgAl-EDDS (L5). To confirm the effect of intercalation with EDTA, the adsorption of metallic ions onto L1 and L2 is also compared. This study investigated the adsorption ability of LDHS as adsorbent for Pb, Cu, and Cd from aqueous solution. Finally, the further

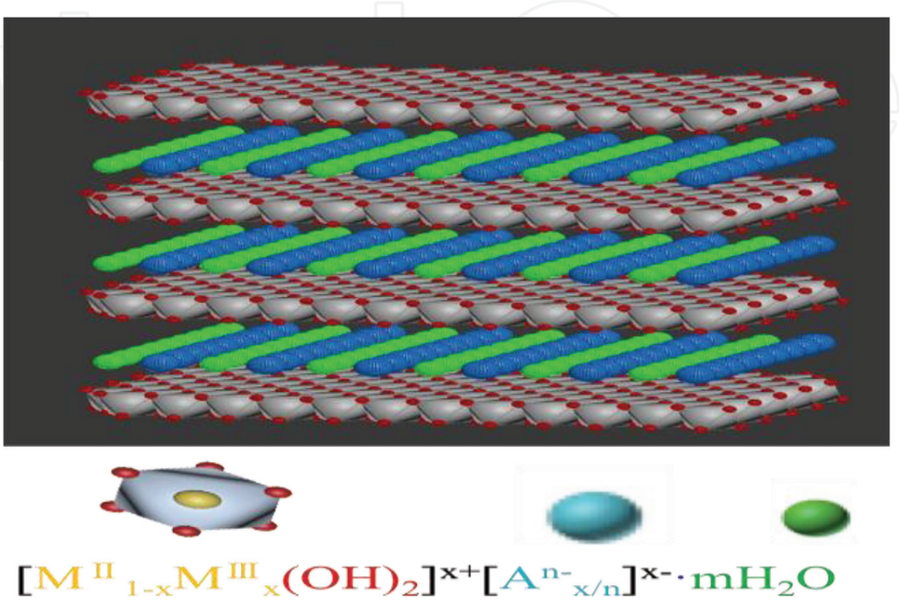

Figure 1.
The layered structure of LDHs.

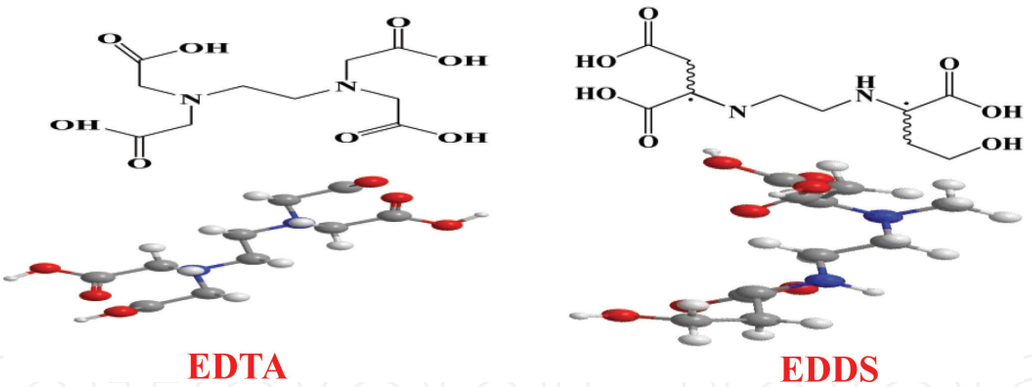

Figure 2.
The structure of EDTA and EDDS.

developments of LDHs as useful adsorbent with the future of application in the environmental chemistry are mentioned.

2. Experimental section

2.1 Materials and reagents

Chemical reagents including $Zn(NO_3)_2{\cdot}6H_2O$, $Al(NO_3)_3{\cdot}9H_2O$, $Mg(NO_3)_2{\cdot}6H_2O$, $Cu(NO_3)_2{\cdot}6H_2O$, $Pb(NO_3)_2$, $Na_2H_2EDTA{\cdot}2H_2O$, NaOH, HNO_3 and Zn(II) Mg(II), and Al(II) standard solution were purchased from Kanto Chemical Co., Inc.; Cd(II) standard solutions were prepared by diluting a standard solution (1000 mg L^{-1}); EDDS (35%) was purchased from Sigma Co., Ltd.; and all reagents used were of analytical grade. CO_2 free water (>18.2 MΩ) which was treated as an ultrapure water system (RFU 424TA, Advantech Aquarius) was employed throughout the work. The pH meter (HORIBA F-72) was used for measurement of pH while adjusting the pH by using 0.01 or 0.1 mol L^{-1} NaOH aqueous solution and 0.01 or 0.1 mol L^{-1} HNO_3 aqueous solution. All synthesis should be performed under a N_2 atmosphere condition to avoid carbonate contamination.

2.2 Synthesis of the adsorbents

The synthesis of LDHs intercalated with EDTA or EDDS includes two steps: (1) the preparation of the precursor LDHs (L1 or L4) and (2) the anion exchange reaction of this compound with chelating agents [14]. All the synthesis was purged with N_2 to avoid CO_2 uptake from atmosphere.

- Synthesis of Precursor L1 and L4

L1 was prepared by dropping addition of 100 mL aqueous solution of 0.02 mol L^{-1} $Zn(NO_3)_2{\cdot}6H_2O$ and 0.01 mol L^{-1}Al $(NO_3)_3{\cdot}9H_2O$ to 100 mL NaOH/$NaNO_3$ solution. Then, the solutions were agitated at 70°C for 8 h by maintaining the pH, separated by centrifugation, and washed until neutral. L4 was also synthesized by using Mg $(NO_3)_2{\cdot}6H_2O$ and Al $(NO_3)_3{\cdot}9H_2O$ as the similar method [15, 16].

- Synthesis of L2, L3, and L5

L2 was synthesized as follows. Under a N_2 atmosphere, 0.015 mol of EDTA or EDDS was added to the 150 mL of suspended solution of L1. Then, the mixing solutions were agitated at 70°C for 8 h under a certain pH degree, then separated by

centrifugation, washed until neutral, and then dried at 60°C overnight [12, 17]. L5 was synthesized by L4 as the similar method for L2.

2.3 Characterization of these adsorbents

Elemental chemical analyses of C, H, and N in LDHs were carried out using an elemental analyzer instrument (JMC10, J-SCIENCE LAB CO., Ltd.). After dissolving the sample by HNO_3, the amount of metallic ions in LDHs was obtained by ICP-MS (Agilent HP 4500, Thermo). Infrared spectra were obtained using the KBr disc method, with wavenumbers from 400 to 4000 cm^{-1} on a FT-IR (FTIR-4200, Jasco, Japan). XRD (X-ray powder diffraction) of LDHs samples were carried out on a RINT2500HR-PC (RIGAKU Corporation) using Cu *K*α radiation in the scanning range of 2–80°. N_2 adsorption and desorption isotherms were employed to determine the specific surface area by the specific surface area analyzers (AUTOSORB-1, Quabtachrome Inc., USA). The surface morphology of LDHs was surveyed using scanning electron microscopy (SEM; JSM-5800, JEOL, Japan). The element distribution and the component analysis were also analyzed by electron probe micro analyzer (EPMA; 1600, Shimadzu Corporation).

2.4 Adsorption experiments

For obtaining the optimum conditions regarding the adsorption of heavy metal, the batch experiments were studied by varying pH, contact time, adsorbent dose, and initial concentration on the adsorption of heavy metal [18–20]. The adsorption experiments of Cu(II) and Pb(II) using L2 and L3 were carried out. A certain amount of L2 or L3 was contacted with 30 mL of an aqueous solution containing known initial each metal ion (nitrate salts) ranging from 0.1 to 2 g L^{-1}. Sorption experiments were conducted in the pH range of 2–6, contact time from 30 minutes to 6 h, temperature from 25 to 40°C, and adsorbent dosage 5–40 mg. The pH of each solution was adjusted using 0.1 mol L^{-1} NH_4OH and 0.1 mol L^{-1} HNO_3. The adsorption capacities of Cu(II) or Pb(II) on L1, L2, and L3 were compared with that of commercial LDHs: DHT-4A ($[Mg_{4.5}Al_2(OH)_{13}CO_3{\cdot}3.5H_2O]$, Kyowa Chemical Industry Co., Ltd), which is abbreviated as L0 below.

The adsorption experiments of Cd(II) were also carried out similar as the method below. The experiment using heavy metallic ions solution without the adsorbent was also performed to identify potential loss of heavy metallic ions during the process such as precipitation. To confirm the effect of intercalation with EDTA, the adsorption of Cu(II), Pb(II) Cd(II) onto L4 and L5 are also compared.

The suspension containing the adsorbent and each of the above metallic solution was filtered through a 0.10 μm membrane filter (Mixed Cellulose Ester 47 mm, Advantec MFS, Inc.) to remove each metallic ion that have been adsorbed into the adsorbent. Then, the concentration of Cu(II) or Pb(II) in the filtrate was determined with an atomic absorption spectrophotometer (AAS), and the concentration of Cd(II) in the filtrate was determined by inductively coupled plasma-atomic emission spectrophotometer (ICP-AES) (SPS 1500, Seiko Instrument Inc).

2.5 Data analysis

For data analysis, various equilibrium, kinetic, and thermodynamic models (equations) were employed to interpret the data and establish the extent of adsorption. The metallic ions uptake by each adsorbent was calculated using the Eq. (1):

$$Q = \frac{(C_0 - C_e)}{W} \cdot V \quad \left[\mu g \cdot g^{-1}\right] \tag{1}$$

where Q is the adsorption capacities at equilibrium (μg g^{-1}), C_o and C_e are the initial and equilibrium concentrations of metallic ions in a batch system, respectively (mg L^{-1}), V is the volume of the solution (L), and W is the weight of each adsorbent (g) [15, 16].

2.6 Adsorption isotherms

In adsorption processes, it is necessary and critical for the equilibrium isotherm studies to predict the behavior of pollutant adsorption onto the sorbent surfaces. Two common adsorption models, Langmuir and Freundlich isotherm models, were applied to evaluate the adsorption data obtained in this study.

The Langmuir adsorption model is based on the assumption that maximum adsorption corresponds to saturated monolayer of solute molecules on the adsorbent surface [21, 22]. Langmuir model is given by Eq. (2):

$$\frac{C_e}{q_e} = \frac{C_e}{q_{\max}} + \frac{1}{K_L q_{\max}} \tag{2}$$

where C_e is the concentration of metallic ions in batch system at equilibrium (mg L^{-1}), q_e is the amount of adsorption of metallic ions at equilibrium (mg g^{-1}), $q_{\max}$ is the maximum adsorption capacity on the surface of adsorbent (mg g^{-1}), and K_L is the equilibrium adsorption constant (L mg^{-1}). A plot of C_e/q_e versus C_e gives a straight line ($Y = A + BX$) with slope of $1/q_{\max}$, and the intercept is $1/(K_L q_{\max})$;

The linearized Freundlich model isotherm is represented by the following equation:

$$\lg q_e = \lg K_F + (1/n) \lg C_e \tag{3}$$

where K_F and $1/n$ indicate the adsorption capacity and the adsorption intensity of the system, respectively. The plots of q_e versus C_e in log scale can be plotted to determine values of $1/n$ and K_F depicting the constants of Freundlich model. The greater the value of the n, the more favorable is the adsorption [15, 16, 23].

2.7 Kinetic model

The kinetic data can be used to determine the time required for adsorption equilibrium and provide useful data to improve the efficiency of the adsorption model and develop predictive models [24, 25]. In this work, pseudo-first-order and pseudo-second-order models were applied for modeling the adsorption process. The pseudo-first-order model is expressed as the Eq. (4):

$$\ln(q_e - q_t) = \ln q_e - k_1 t \tag{4}$$

where q_t and q_e (μg g^{-1}) are the metal amount adsorbed at time at t (h) and equilibrium, respectively, and k_1 is the rate constant of the pseudo-first-order adsorption (h^{-1}).

The linear form of the pseudo-second-order rate equation is given as follows:

$$\frac{t}{q_t} = \frac{1}{k_2 q_e^2} + \frac{t}{q_e} \tag{5}$$

where k_2 (g μg^{-1} h^{-1}) is the pseudo-second-order rate constant of the adsorption [15, 16, 25].

3. Results and discussion

3.1 Chemical analysis

The chemical analysis of LDH samples is shown in **Table 1**. The molar ratio of M^{II}/M^{III} in L1 or L4 is nearly 2 which is well fitted to the expected formula. However, L2, L3, or L5 has lower M^{II}/M^{III} ratio than L1 or L4. The presence of polydentate ligand (Zn-EDTA or Al-EDTA complex) can result in this decrease of the ratio. Moreover, the decrease suggests that octahedron in hydroxyl layer has a partial dissolution (pK_{sp} ($Zn(OH)_2$) = 13.7, pK_{sp} ($Al(OH)_3$) = 32.7, pK_{sp} ($Mg(OH)_2$) = 12.7) during the anion exchange reaction which is performed at pH 5–6 [12, 17, 26]. The C/N of L5 is lower than that of EDTA ligand (5), and the little gap between them may be mainly due to the registration of nitrate ions in the interlayer. The more nitrate ions are included in LDHs, the lower the C/N value is [27].

3.2 FT-IR spectra

The FT-IR spectra of L1 and L2 and L3 are shown in **Figure 3**, and that of L4 and L5 are shown in **Figure 4**. Typical M-OH (M—metallic ions) vibration modes due to the hydroxide layer between 400 and 1000 cm^{-1} are found in both **Figures 3** and **4**.

The very sharp peak at 1385 cm^{-1} in **Figures 3(a)** and **4(a)** is attributed to the NO_3^- stretching vibration. The NO_3^- stretching vibration at 1385 cm^{-1} is not observed from **Figures 3(b)** to **4(b)**. It may be due to the group which is hidden by the band at 1394 cm^{-1} [26, 28]. The absorption bands at 1600 and 1394 cm^{-1} are characteristics of the symmetrical and asymmetrical vibration of COO- groups. The position of these bonds is similar to the spectrum of LDHs which is reported by Parida et al. [29] and [30]. It is found that EDTA has been intercalated into the interlayer successfully, although a certain amount of -NO_3 may still retain in the compound judging from the results of chemical analysis. The wide band at around 3450 cm^{-1} may be attributed to the -H bonding stretching vibrations of -OH groups and water molecules. The band at 1623 cm^{-1} of L1 and L4 is assigned to water bending vibration [8, 26].

3.3 XRD patterns

XRD patterns of L1 and L2 and L3 are shown in **Figure 5**, and those of L4 and L5 are shown in **Figure 6**. They are typical XRD patterns of LDHs. The strong diffraction peaks at low angle, assigned to basal planes (003), (006), (009), were sharp and symmetric compared to the peaks at high angle, which are characteristics of clay mineral

	wt%	N	H	Atomic ratios			Proposed formula
		C		M^{II}/M^{II}	C/H	H/N	
L1	0.54	5.17	3.24	2.23	0.01	8.79	$[Mg_2Al(OH)_6]NO_3$
L2	11.2	3.83	4.19	1.88	0.22	20.1	$[Mg_2Al(OH)_6]_2[C_{10}H_{14}N_20_8]$
L3	9.82	2.21	4.15	1.79	0.20	26.3	$[Mg_2Al(OH)_6]_2[C_{10}H_{13}N_2Na0_8]$
L4	0.06	4.26	2.38	2.10	0.00	7.82	$[Zn_2Al(OH)_6]NO_3$
L5	13.7	3.35	3.60	1.67	0.31	15.1	$[Zn_2Al(OH)_6]_2$ $[C_{10}H_{14}N_20_8]$

Table 1.
Chemical analysis results of L1, L2, L3, L4, and L5.

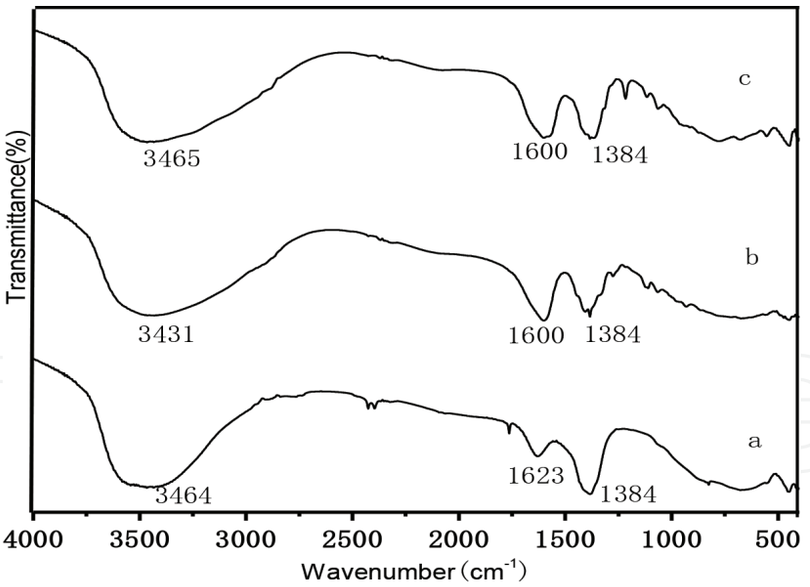

Figure 3.
FT-IR spectra of (a) L1, (b) L2, and (c) L3.

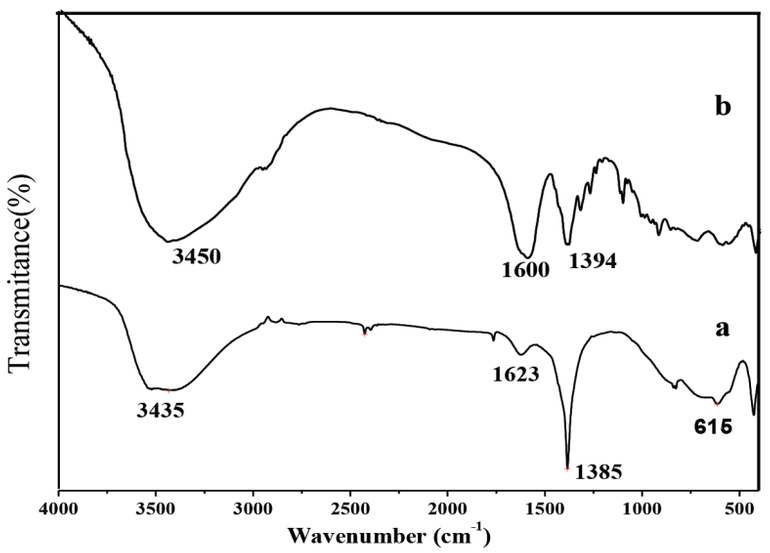

Figure 4.
FT-IR spectra of (a) L4 and (b) L5.

shaving a layered structure [29–31]. From the XRD pattern, the basal spacing (d) values of sample were calculated by using Bragg equation and the angle of peak (003).

Then the gallery height was obtained by subtraction from the basal spacing to the layer width (0.48 nm) [30]. The basal spacing and the gallery height of L1, L2, L4, and L5 are shown in **Table 2**. It indicates that the intercalation of EDTA into NO_3-LDHs gives rise to an increase of basal spacing. This basal spacing could identify the existence of EDTA, because it is close to the dimensions of EDTA complexes (0.9 nm^{-1} nm) founded by single crystal XRD of M-EDTA (M—metallic ions) compound [12, 17, 30, 32].

3.4 SEM micrographs

SEM images of all composite synthesized in this work are shown in **Figure 7**. These adsorbents have clear plate-like morphology, which is typical for LDHs [33]. The intercalated product particles are more homogeneous than the precursor product

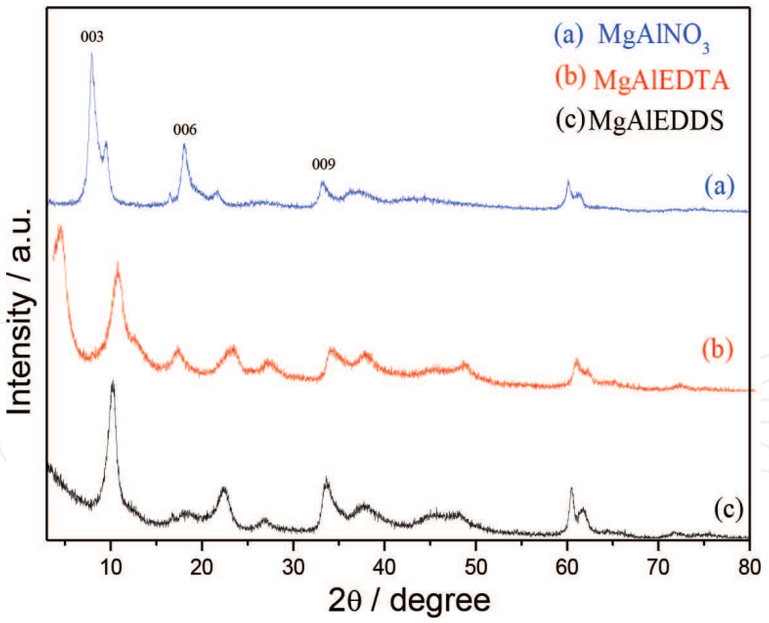

Figure 5.
XRD patterns of (a) L1, (b) L2, and (c) L3.

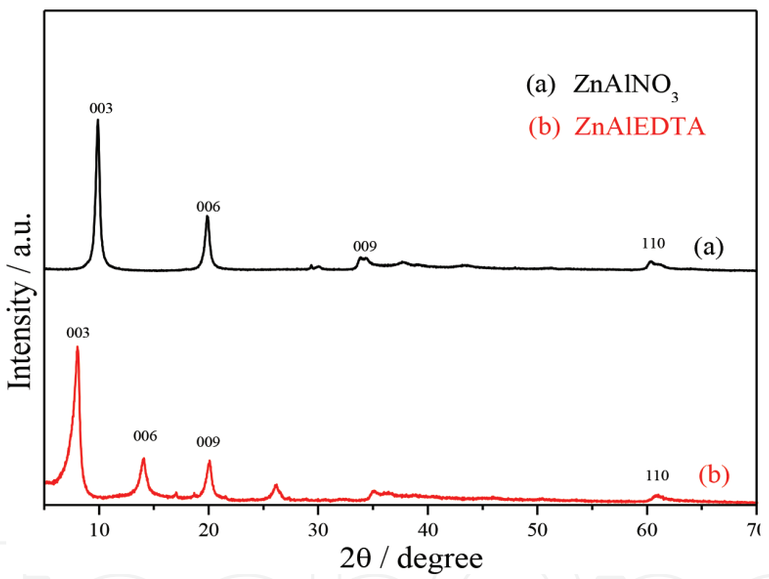

Figure 6.
XRD patterns of (a) L4 and (b) L5.

	L1	L2	L4	L5
Basal spacing	0.91	1.42	0.89	1.47
Gallery height	0.43	0.94	0.41	0.99

Table 2.
The basal spacing of L1, L2, L4, and L5 calculated from XRD by using Bragg's equation.

which may be due to the hydrogen bonding on the layer. Hydrogen bonding makes soft agglomeration occur on the surface of the LDHs, and after the chelating agent, anion replaces the nitrate ions between the layers, the hydrogen bonding between the hydroxyl groups is reduced, and the aggregation is weakened to a certain extent.

The inhomogeneous surface of the adsorbent indicated that a large amount of metal salt attached to the surface of the hydrotalcite in an excessive state, its unique

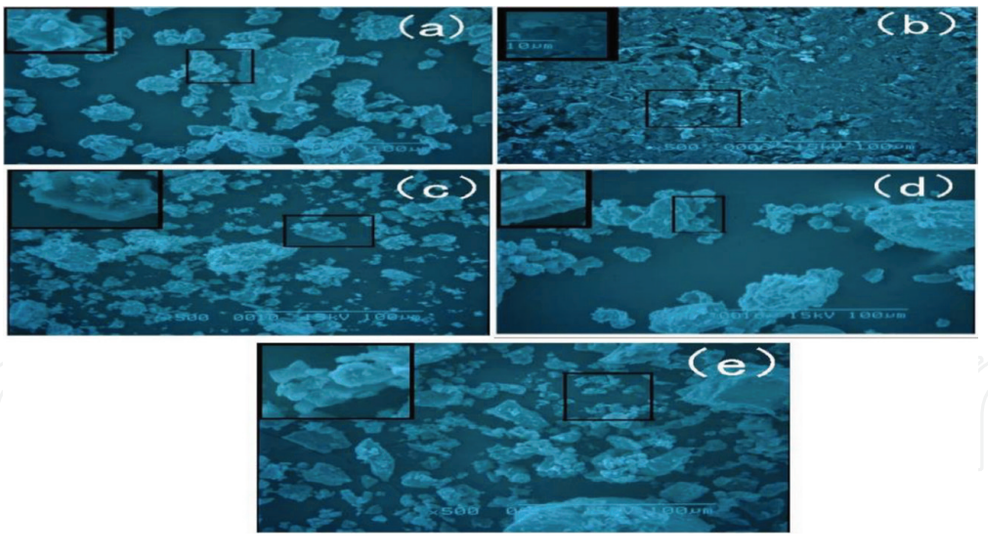

Figure 7.
SEM image of (a) L1, (b) L2, (c) L3, (d) L4, and (e) L5.

layered structure, resulting in removal of heavy metal ions in the aqueous solution not only by interlayer anion and heavy metal cation interaction but also rely on the role of surface adsorption and sedimentation.

3.5 Electron probe microanalyzer (EPMA)

Element distribution analysis of L1, L2, L4, and L5 by EPMA is shown in **Figure 8**. After the ion exchange, the element distribution of N decreased obviously (by comparing red parts in these pictures), and this decrease is observed in both MgAl-LDHs (a, b) and ZnAl-LDHs (c, d). Furthermore, it is found that the moles of divalent metals are at least equal to or greater than that of the trivalent metals [34, 35], which is consistent with the results of chemical analysis.

3.6 Specific surface area

Figure 9 has shown the specific surface area of the product. Specific surface area of L2 and L3 are bigger than that of L1, and that of L5 is bigger than L4, which may be attributed to intercalation of EDTA or EDDS. Specific surface area of L0 is bigger than that of L1; it is due to the difference of their particle size.

3.7 Adsorption of Cu(II) or Pb(II) onto L1, L2, L3, and L0

The adsorption capacities of Cu(II) or Pb(II) onto L1, L2, L3, and L0 are compared in **Figure 10**. The adsorption efficiency of Cu^{2+} was larger than that of Pb^{2+} for the same absorbent, which could be attributed to their stability constant (EDTA-Cu, 18.7; EDDS-Cu, 18.4; EDTA-Pb, 18.0; EDDS-Pb, 12.7) [12, 26]. That is to say, it can be considered that the large adsorption capacity is obtained when the stability constant of chelate-metal is high. By comparing among adsorbents used in this work, the order of the adsorption capacity is L2 > L3 > L0 > L1. The higher adsorption efficiency of L0 than L1 may be attributable to its high specific surface area.

3.8 Adsorption of Cu(II), Pb(II), and Cd(II) onto L4 and L5

In order to confirm the effect of the intercalation with chelate agents on the adsorption capacity of metals, the adsorption experiments of some metallic elements

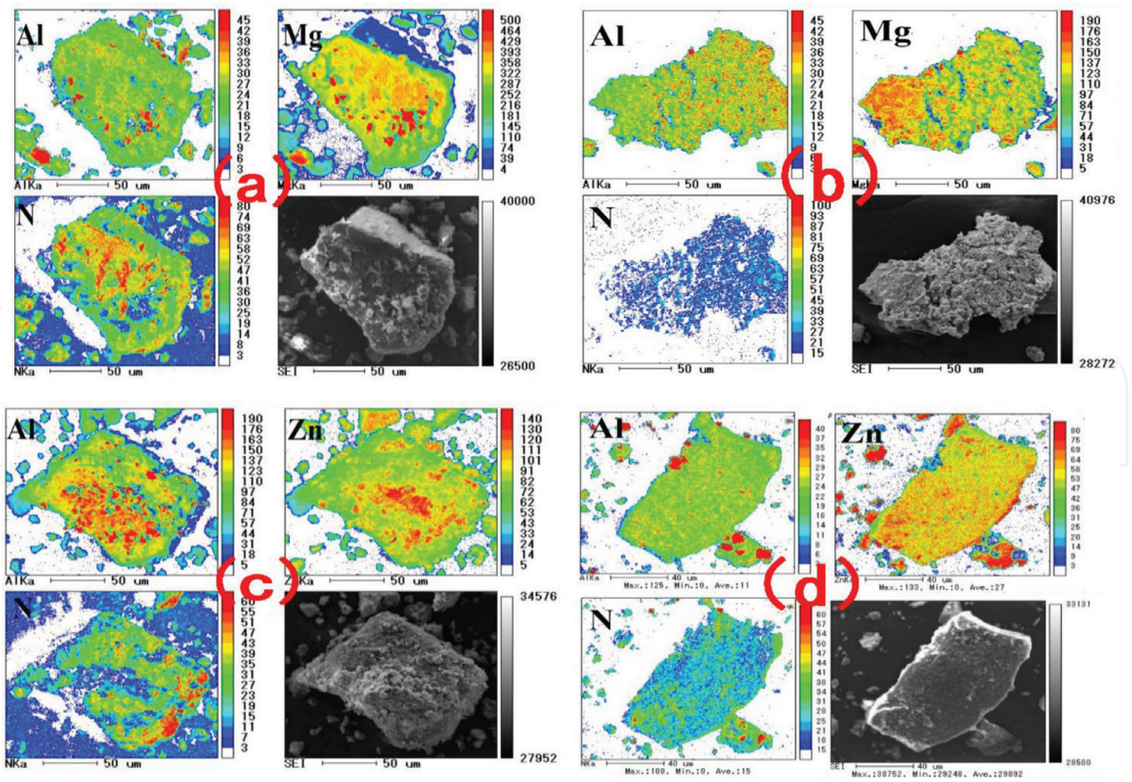

Figure 8.
Element distribution analyzed by EPMA of (a) L1, (b) L2, (c) L4, and (d) L5.

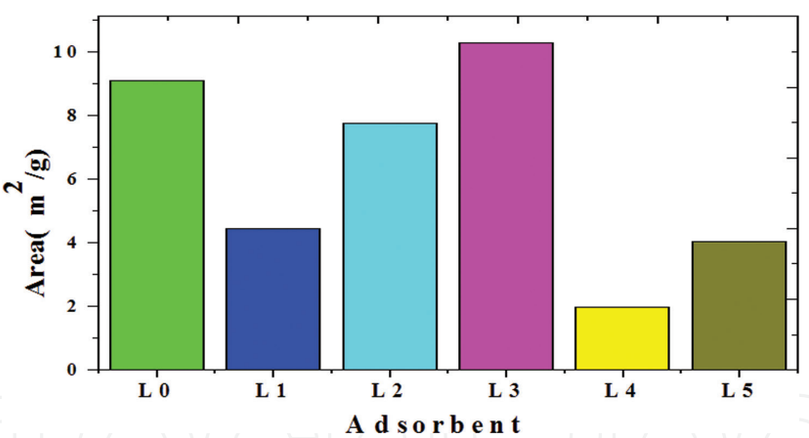

Figure 9.
Specific surface area of L0, L1, L2, L3, L4, and L5 by BET method.

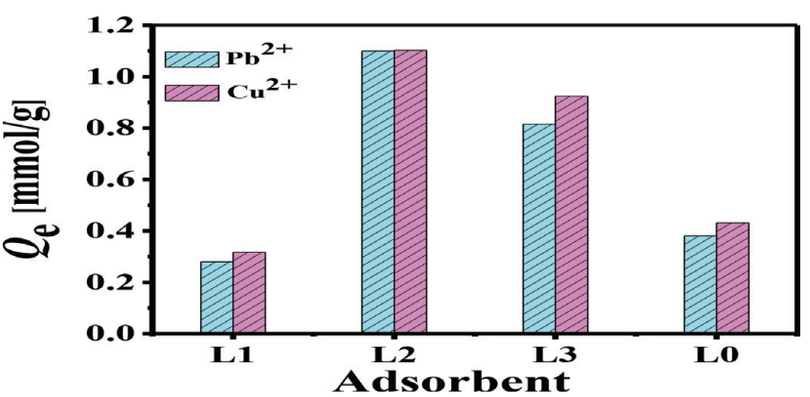

Figure 10.
The adsorption capacity of Pb^{2+} and Cu^{2+} onto L1, L2, L3, and L0.

onto L1 and L2 are compared. The adsorption of Cd(II), Cu(II), and Pb(II) onto these LDHs under the optimum condition are shown in **Figures 11–13**, respectively.

Both LDHs were found to take up Cd(II), Cu(II), and Pb(II) from aqueous solutions, and the uptake was found to increase with time. The adsorption capacity of both LDHs for Cd(II), Cu(II), and Pb(II) increased rapidly during the initial stages, and thereafter it increased gradually. It is generally found that the time needed for L5 to reach equilibrium was shorter than that for L4. From the adsorption experiment, the improvement of adsorption capacity by intercalation was observed. On the other hand, the adsorption capacity of Cu(II) and Pb(II) at equilibrium was

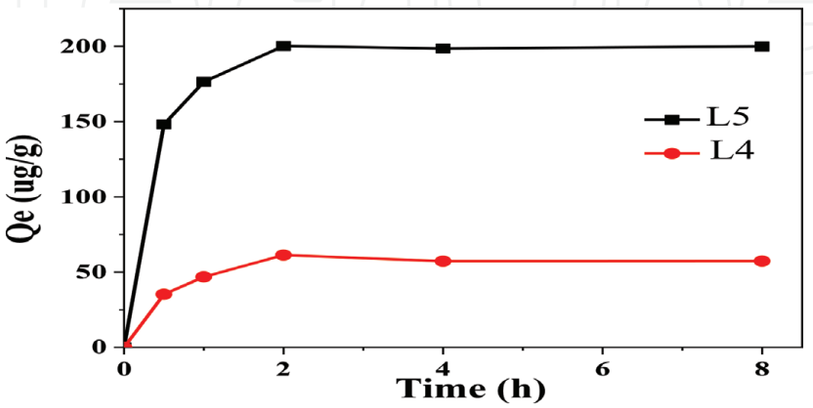

Figure 11.
Adsorption of Cd(II) onto L4 and L5.

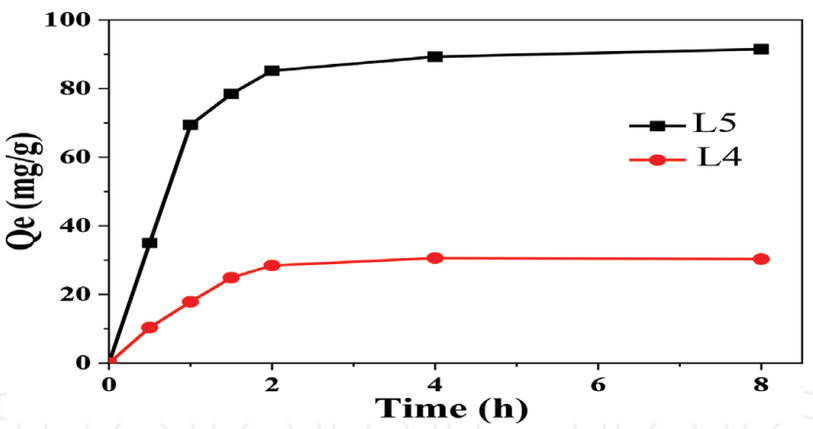

Figure 12.
Adsorption of Cu(II) onto L4 and L5.

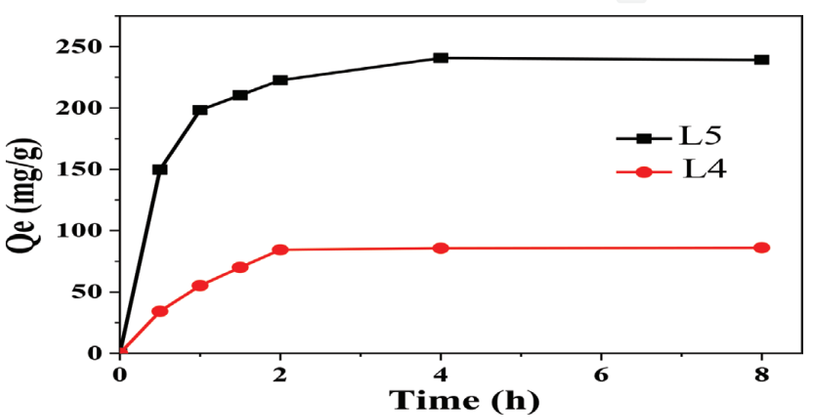

Figure 13.
Adsorption of Pb(II) onto L4 and L5.

higher than that of Cd(II). It is considered that heavy metal was removed by LDHs including two mechanisms: chemical precipitation and chelation [16]. In the first case, the hydroxyl anions compete with chelating agents for the precipitation of metal hydroxides at higher pH, and divalent ions are usually selectively dissolved. In the second case, the adsorption affinity is generally determined by the stability constant of the corresponding complex [36–38].

3.9 Adsorption isotherms

The adsorption isotherms for Cu(II) or Pb(II) were obtained under the optimum adsorption conditions (i.e., pH 6, contact time 120 minutes, temperature 25°C, and adsorbent dosage 10 mg). The adsorption isotherms of Cu(II) or Pb(II) onto L2 and L3 were analyzed using Langmuir and Freundlich equations and were shown in **Figures 14** and **15**, respectively. From **Figure 14**, the linear correlation coefficient (R^2) of L2 (Pb^{2+}), L3 (Pb^{2+}), L2 (Cu^{2+}), and L3 (Cu^{2+}) and other parameter for Langmuir and Freundlich isotherms model were shown in **Table 3**, respectively. That is, L2 and L3 synthesized in this work are well fitted by Freundlich adsorption isotherms models.

3.10 Kinetic model

The kinetic isotherms for Cu(II) or Pb(II) were obtained under the optimum adsorption conditions (i.e., pH 6, concentration 200 ppm, temperature 25°C and

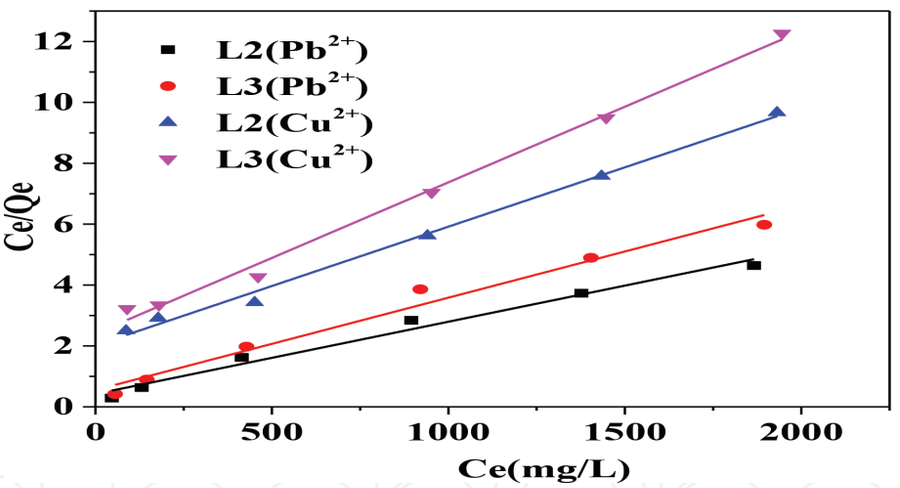

Figure 14.
The correlation of experimental data to Langmuir isotherm models.

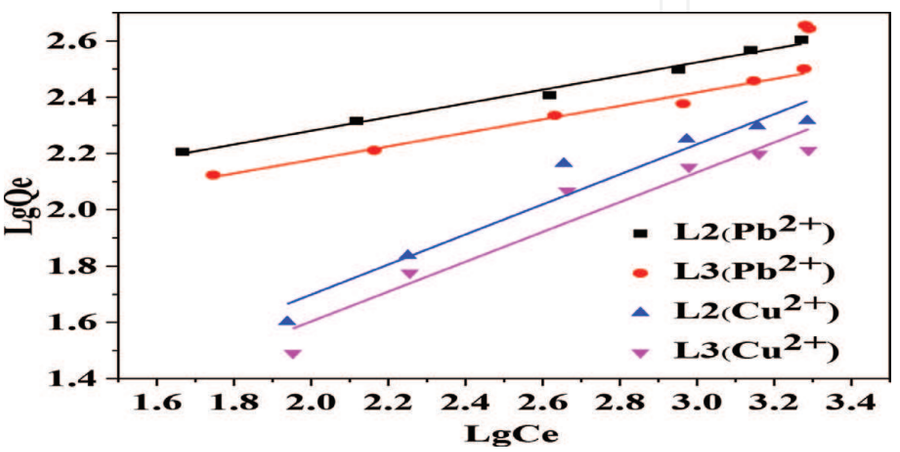

Figure 15.
The correlation of experimental data to Freundlich isotherms models.

Sample/T (298 K)	Langmuir			Freundlich		
	R^2	K_L (L^{-1} mg^{-1})	q_{max} (mg g^{-1})	R^2	K_F ($mg^{1-1/n}$ g^{-1} L^{-1})	n
L2(Pb^{2+})	0.979	5.60×10^{-3}	422	0.988	346	4.11
L3(Pb^{2+})	0.976	5.40×10^{-3}	330	0.983	199	4.17
L2(Cu^{2+})	0.994	1.90×10^{-3}	256	0.930	9.90×10^{-3}	1.87
L3(Cu^{2+})	0.993	2.10×10^{-3}	201	0.914	2.20×10^{-3}	1.89

Table 3.
Coefficient of Langmuir and Freundlich isotherms for Cu(II) and Pb(II) adsorption onto L2 or L3.

adsorbent dosage 10 mg). The parameters for two kinetic models of adsorption of Cu(II) or Pb(II) on L2 or L3 are presented in **Table 4** which showed that adsorption process followed pseudo-second-order rather than pseudo-first-order model.

The second order kinetic models plot for the adsorption of Cu(II) or Pb(II) on L2 or L3 is shown in **Figure 16**. The experimentally calculated values of q_e at various concentrations were in a good agreement with theoretical calculated values. Also, the values of correlation coefficients (R^2) for the pseudo-second-order kinetic model was nearly 1, indicated that pseudo-second-order kinetic model was better obeyed.

3.11 Comparison of the adsorption capacities of the materials with other sorbents

The comparison of maximum adsorption capacity of these LDHs for Cu(II) in a present study with that of another adsorbents in previous literatures [39] are

Sample/T (298 K)	$q_{e\,EXP}$ (mg g^{-1})	Pseudo-first-order			Pseudo-second-order		
		R^2	q_e (mg g^{-1})	K_1 (h^{-1})	R^2	q_e (mg g^{-1})	K_2 (g mg^{-1} h^{-1})
L2(Pb^{2+})	228	0.990	217	5.48	0.997	276	2.75
L3(Pb^{2+})	169	0.940	169	5.27	0.993	229	1.25
L2(Cu^{2+})	71	0.983	78.5	4.35	0.991	111	0.104
L3(Cu^{2+})	59	0.983	54.8	4.09	0.995	91.9	0.910

Table 4.
The kinetic fit parameters for Cu(II) and Pb(II) adsorbed on L2 or L3.

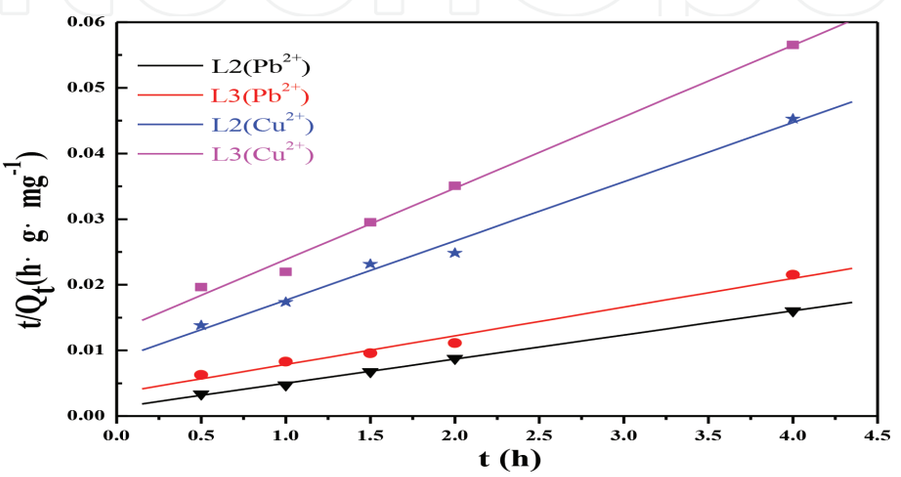

Figure 16.
The correlation of experimental data to pseudo-second-order models.

Adsorbents	Q (mg g^{-1})	References
LS-LDH: MgAl-LDH intercalated by sulfonated lignin (LS)	64	[39]
TA-HTC: hydrotalcite modified by tannin	81	[40]
CL-LDH: LDHs intercalated by chloride	38	[41]
H100-LDH: MgAl-LDH intercalated by humate anions	85	[12]
Sx-LDH: MgAl-LDH intercalated by polysulfide	127	[42]
L0 (MgAl-CO_3)	28	This study
L1 (MgAl-NO_3)	20	This study
L2 (MgAl-EDTA)	71	This study
L3 (MgAl-EDDS)	59	This study
L4 (ZnAl-NO_3)	31	This study
L5 (ZnAl-EDTA)	90	This study

Table 5.
Comparison of the adsorption capacities of LDHs in other literature Cu^{2+}.

Adsorbents	Q (mg g^{-1})	References
MNP-CTS—MNPs modified with chitosan (CTS)	140	[43]
CL-LDH—LDHs intercalated by chloride	40	[16]
CDpoly-MNPs—(CM-β-CD) polymer-modified Fe_3O_4 nanoparticles	65	[44]
H100-LDH—MgAl-LDH intercalated by humate anions	99	[12]
MoS_4-LDH—LDHs intercalated with the MoS_4^{2-} ion	290	[45]
L0 (MgAl-CO_3)	78	This study
L1 (MgAl-NO_3)	58	This study
L2 (MgAl-EDTA)	228	This study
L3 (MgAl-EDDS)	169	This study
L4 (ZnAl-NO_3)	80	This study
L5 (ZnAl-EDTA)	223	This study

Table 6.
Comparison of the adsorption capacities of LDHs in other literature Pb^{2+}.

presented in **Table 5**. Moreover, **Table 6** shows the comparison of adsorption capacity of Pb(II) by other adsorbents reported in the literature. As seen in **Tables 5** and **6**, the adsorption capacity of these LDHs for Cu(II) and Pb(II) in this work is on a level with that of another adsorbents in previous works.

4. Conclusions

In present study, LDHs intercalated with chelating agents have been extensively examined and applied for adsorption of aqueous containing heavy metals and REEs. The following five kinds of compounds were synthesized (MgAl-NO_3 (L1), MgAl-EDTA (L2) and MgAl-EDDS (L3), ZnAl-NO_3 (L4), ZnAl-EDTA (L5)). These

five kinds of synthesized samples are characterized by some instruments and the adsorption capacities of LDHs intercalated with chelating agents for Cu(III), Pb(III), and Cd(III), and REEs ions were investigated by batch experiments. Influence of various condition including pH, adsorbents dose, concentration of metallic ions, adsorption time, and temperature on the removal of metallic ions was evaluated. The Langmuir and Freundlich models were used for the mathematical description of the adsorption isotherms. The suitability of the kinetic model for the adsorption processes is also discussed. The following matters were suggested from the experimental results:

1. In present study, the precursor LDHs ($ZnAl\text{-}NO_3$ and $MgAl\text{-}NO_3$) were intercalated with the chelating agent EDTA (ethylenediaminetetraacetic acid) and EDDS (N, N′-1, 2-Ethanediylbis-1-Aspartic Acid) by anion exchange. The obtained material was characterized and used for the removal of heavy metallic ions and REEs removal from aqueous solutions. The result from FT-IR etc. suggests that the intercalation into LDHs is performed successfully.

2. LDHs synthesized in this work were very effective for removing heavy metallic ions from water solutions. Higher adsorption efficiency is obtained by intercalating chelating agent (i.e., EDTA or EDDS) into LDHs. It is considered that the adsorption capacity of metallic ions onto LDHs is based on the stability constant of metal-chelating agents. For example, the adsorption efficiency of Cu(III) was higher than that of Pb(III) for the same absorbent.

3. Adsorption isotherms of adsorption data were studied at varying initial concentration of metallic ions under optimized conditions of contact time and the dosage of adsorbents in this work. The adsorption experimental data of heavy metallic ions onto LDHs were well fitted by the Freundlich adsorption isotherms model. The results suggest that LDHs synthesized in this work could be suitable as sorbent materials for the adsorption and removal of heavy metal ions from aqueous solutions.

4. The pseudo-first-order kinetic and pseudo-second-order models were applied to test the experimental data and explain the kinetics of the LDHs adsorption process. The comparison of evaluated correlation coefficients suggested that the pseudo-second-order model is most suitable for describing the adsorption processes. The confirmation of this model implies that the rate-limiting step in this adsorption system may be controlled by chemical process. Also, the concentrations of both adsorbent and adsorbate are associated with the rate determining step of the adsorption process.

From this work, it was quantitatively clarified that LDHs could be an efficient adsorbent for heavy metal. It is a very significant information from the viewpoint of environmental protection and can be used for treating industrial waste waters including pollutants and thus a promising option for the treatment of contaminated waters.

Acknowledgements

The present work was partially supported by a Grant-in-Aid for Scientific Research from the Japan Society for the Promotion of Science (Research Program(C), no. 16K00599) and a fund for the promotion of Niigata University

KAAB Projects from the Ministry of Education, Culture, Sports, Science and Technology, Japan. The authors are also grateful to Mr. M. Ohizumi of the Office for Environment and Safety in Niigata University, Dr. E. Tayama of Faculty of Science, Dr. M. Teraguchi, Mr. T. Nomoto, Prof. T. Tanaka, and Mr. T. Hatamachi of Faculty of Engineering and Mr. M. Kobayashi of Facility of Dentistry in Niigata University for permitting the use of ICP-AES, elemental analyzer, FT-IR, SEM, specific surface area analyzers, and EPMA and for giving helpful advice in measurement.

Author details

Naoki Kano[1*] and Shuang Zhang[2]

1 Department of Chemistry and Chemical Engineering, Niigata University, Niigata, Japan

2 Graduate School of Science and Technology, Niigata University, Niigata, Japan

*Address all correspondence to: kano@eng.niigata-u.ac.jp

References

[1] Dutta S, Das AK. Analytical perspective on waste management for environmental remediation. Trends in Analytical Chemistry. 2010;**29**(7):636-644

[2] Sanchez A, Recillas S, Font X, et al. Ecotoxicity of, and remediation with, engineered inorganic nanoparticles in the environment. Trends in Analytical Chemistry. 2011;**30**(3):507-516

[3] Faraji M, Yamini Y, Rezaee M. Magnetic nanoparticles: Synthesis, stabilization, functionalization, characterization, and applications. Journal of the Iranian Chemical Society. 2010;**7**(1):1-37

[4] He M, Hu B, Zeng Y, Jiang Z. ICP-MS direct determination of trace amounts of rare earth impurities in various rare earth oxides with only one standard series. Journal of Alloys and Compounds. 2005;**390**:168-174

[5] Amirianshoja T, Junin R, Idris AK, Rahmani O. A comparative study of surfactant adsorption by clay minerals. Journal of Petroleum Science and Engineering. 2013;**101**:21-27

[6] Hatch CD, Wiese JS, Crane CC, et al. Water adsorption on clay minerals as a function of relative humidity: Application of BET and Freundlich adsorption models. Langmuir. 2012;**28**:1790-1803

[7] Zhao P, Liu X, Tian W, et al. Adsolubilization of 2, 4, 6-trichlorophenol from aqueous solution by surfactant intercalated ZnA layered double hydroxides. Chemical Engineering Journal. 2015;**279**:597-604

[8] Jiao FP, Chen XQ, Liu L, Hu ZD, Hu YH, Wang YH. Preparation and characterization of Mg-Al/Zn-Al layered double hydroxides intercalated with (+)-2, 3-di(p-toluyl)-tartaric acid. Journal of Molecular Structure. 2010;**964**(1):152-157

[9] Zhang H, Zou K, Guo SH, Duan X. Nanostructural drug-inorganic clay composites: Structure, thermal property and in vitro release of captopril-intercalated Mg-Al-layered double hydroxides. Journal of Solid State Chemistry. 2006;**179**(6):1792-1801

[10] Gyliene O, Aikaite J, Nivinskien O. Recovery of EDTA from complex solution using Cu(II) as precipitant and Cu(II) subsequent removal by electrolysis. Journal of Hazardous Materials. 2004;**116**(1):119-124

[11] Prieto C, Lozanoa JC, Rodríguez PB, Tome FV. Enhancing radium solubilization in soils by citrate, EDTA, and EDDS chelating amendments. Journal of Hazardous Materials. 2013;**250**:439-446

[12] Perez MR, Pavlovic I, Barriga C, et al. Uptake of Cu^{2+}, Cd^{2+} and Pb^{2+} on Zn-Al layered double hydroxide intercalated with EDTA. Applied Clay Science. 2006;**32**(3):245-251

[13] Gonzalez MA, Pavlovic I, Rojas R, Barriga C. Removal of Cu^{2+}, Pb^{2+} and Cd^{2+} by layered double hydroxide-humate hybrid. Sorbate and sorbent comparative studies. Chemical Engineering Journal. 2014;**254**:605-611

[14] Kaneyoshi M, Jones W. Formation of Mg-Al layered double hydroxides intercalated with nitrilotriacetate anions. Journal of Materials Chemistry. 1999;**9**:805

[15] Sui MH, Zhou YF, Sheng L, Duan BB. Adsorption of norfloxacin in aqueous solution by Mg-Al layered double hydroxides with variable metal composition and interlayer anions. Chemical Engineering Journal. 2012;**210**:451-460

[16] Liang XF, Hou WG, Xu YM, et al. Sorption of lead ion by layered double hydroxide intercalated with diethylenetriaminepentaacetic acid. Colloids and Surfaces A: Physicochemical and Engineering Aspects. 2010;**366**(1):50-57

[17] Escudero C, Gabaldon C, Marzal P, Villaescusa L. Effect of EDTA on divalent metal adsorption onto grape stalk and exhausted coffee wastes. Journal of Hazardous Materials. 2008;**152**:476-485

[18] Zhang S, Kano N, Imaizumi H. Adsorption of Cu(II), Pb(II) by Mg-Al layered double hydroxides (LDHs): Intercalated with the chelating agents EDTA and EDDS. Journal of Chemical Engineering of Japan. 2014;**47**(4):324-328

[19] Zhang S, Kano N, Imaizumi H. Adsorption of Cd(II) on Zn-Al LDHs (layered double hydroxides) intercalated with chelating agents EDTA. Journal of Chemistry and Chemical Engineering. 2016;**10**(2):60-67

[20] Zhang S, Kano N, Imaizumi H. Synthesis and characterization of LDHs (layered double hydroxides) intercalated with EDTA (ethylenediaminetetracetic acid) or EDDS (N, N'-1, 2-ethanediylbis-1-aspartic acid). Journal of Environmental Science and Engineering A. 2016;**5**:549-558

[21] Won SW, Choi SB, Yun YS. Performance and mechanism in binding of reactive orange 16 to various types of sludge. Biochemical Engineering Journal. 2006;**28**:208-214

[22] Wang B, Guo X, Peng B. Removal technology of boron dissolved in aqueous solutions—A review. Colloids and Surfaces A: Physicochemical and Engineering Aspects. 2014;**444**:338-344

[23] Ayawei N, Ekubo AT, Wankasi D, Dikio ED. Synthesis and application of layered double hydroxide for the removal of copper in wastewater. International Journal of Chemistry. 2015;**7**(1):122-132

[24] Ayawei N, Ekubo AT, Wankasi D, Dikio ED. Adsorption dynamics of copper adsorption by Zn/Al-CO_3. IJACSA. 2015;**3**(1):57-64

[25] Dolatyari L, Yaftian MR, Rostamnia S. Adsorption characteristics of Eu(III) and Th(IV) ions onto modified mesoporous silica SBA-15 materials. Journal of the Taiwan Institute of Chemical Engineers. 2016;**60**:174-184

[26] Gasser MS, Aly HF. Kinetic and adsorption mechanism of Cu(II) and Pb(II) on prepared nanoparticle layered double hydroxide intercalated with EDTA. Colloids and Surfaces A: Physicochemical and Engineering Aspects. 2009;**336**(1-3):167-173

[27] Rives V. Layered Double Hydroxides: Present and Future. New York: Nova Publishers; 2001

[28] Chitrakar R, Tezuka S, Sonoda A, et al. Synthesis and phosphate uptake behavior of Zr^{4+} incorporated MgAl-layered double hydroxides. Journal of Colloid and Interface Science. 2007;**313**:53-63

[29] Parida KM, Baliarsingh N, Sairam PB, Das J. Copper phthalocyanine immobilized Zn/Al LDH as photocatalyst under solar radiation for decolorization of methylene blue. Journal of Molecular Catalysis A: Chemical. 2006;**267**(1):202-208

[30] Park M, Choi CL, Seo YJ, et al. Reactions of Cu^{2+} and Pb^{2+} with Mg/Al layered double hydroxide. Applied Clay Science. 2007;**37**(1):143-148

[31] Cavani F, Trifirb F, Vaccari A. Hydrotalcite type anionic

clays: Preparation, properties and applications. Catalysis Today. 1991;**11**(2):173-301

[32] Rojas R. Copper, lead and cadmium removal by Ca Al layered double hydroxides. Applied Clay Science. 2014;**87**:254-259

[33] Osama S, Hideyuki T. Preparation and intercalation reactions of nano-structural materials, Zn-Al-Ti LDH. Materials Chemistry and Physics. 2008;**108**(2):449-455

[34] Zhang CL, Yu JY, Xu S, Xue LH, Cao ZL. Influence of UV aging on the rheological properties of bitumen modified with surface organic layered double hydroxides. Construction and Building Materials. 2016;**123**:574-580

[35] Liang XF, Zang YB, Xu YY, et al. Sorption of metal cations on layered double hydroxides. Colloids and Surfaces A: Physicochemical and Engineering Aspects. 2013;**433**:122-131

[36] Buxbaum G, Pfaff G. Cadmium Pigments. Industrial Inorganic Pigments. Hoboken, New Jersey, USA: Wiley-VCH; 2005. pp. 121-123

[37] Morrow H. Cadmium and Cadmium Alloys, Kirk-Othmer Encyclopedia of Chemical Technology. Hoboken, New Jersey, USA: John Wiley & Sons; 2010. pp. 1-36

[38] Kameda T, Saito S, Umetsu Y. Mg-Al layered double hydroxide intercalated with ethylene diaminetetraacetate anion: Synthesis and application to the uptake of heavy metal ions from an aqueous solution. Separation and Purification Technology. 2005;**47**(1):20-26

[39] Huang G, Wang D, Ma S, Chen J, Jiang L, Wang P. A new, low-cost adsorbent: Preparation, characterization, and adsorption behavior of Pb(II) and Cu(II). Journal of Colloid and Interface Science. 2015;**445**:294-302

[40] Anirudhan TS, Suchithra PS. Synthesis and characterization of tannin-immobilized hydrotalcite as a potential adsorbent of heavy metal ions in effluent treatments. Applied Clay Science. 2008;**42**:214-223

[41] Gonzalez MA, Pavlovic I, Barriga C. Cu(II), Pb(II) and Cd(II) sorption on different layered double hydroxides. A kinetic and thermodynamic study and competing factors. Chemical Engineering Journal. 2015;**269**:221-228

[42] Ma S, Chen Q, Li H, Wang P, Islam SM, Gu Q, et al. Highly selective and efficient heavy metal capture with polysulfide intercalated layered double hydroxides. Journal of Materials Chemistry A. 2014;**2**:10280-10289

[43] Zhou L, Ji L, Ma P-C, Shao Y, Zhang H, Gao W, et al. Development of carbon nanotubes/$CoFe_2O_4$ magnetic hybrid material for removal of tetrabromobisphenol A and Pb(II). Journal of Hazardous Materials. 2014;**265**:104-114

[44] Badruddoza AZM, Shawon ZBZ, Daniel TWJ, Hidajat K, Uddin MS. Fe_3O_4/cyclodextrin polymer nanocomposites for selective heavy metals removal from industrial wastewater. Carbohydrate Polymers. 2013;**91**:322-332

[45] Ma L, Wang Q, Islam SM, Liu Y, Ma S, Kanatzidis MG. Highly selective and efficient removal of heavy metals by layered double hydroxide intercalated with the MoS_4^{2-} ion. JACS. 2016;**138**:2858-2866